Carcinogenesis vol.31 no.3 pp.504–511, 2010
doi:10.1093/carcin/bgp313
Advance Access publication December 16, 2009

IQGAP1 and vimentin are key regulator genes in naturally occurring hepatotumorigenesis induced by oxidative stress

Akihito Tsubota*, Kenji Matsumoto[1], Kaoru Mogushi[2], Koichi Nariai, Yoshihisa Namiki, Sadayori Hoshina, Hiroshi Hano[3], Hiroshi Tanaka[2], Hirohisa Saito[1] and Norio Tada

Institute of Clinical Medicine and Research, Jikei University School of Medicine, 163-1 Kashiwa-shita, Kashiwa, Chiba 277-8567, Japan, [1]Department of Allergy and Immunology, National Research Institute for Child Health and Development, 2-10-1 Okura, Setagaya-ku, Tokyo 157-8535, Japan, [2]Information Center for Medical Sciences, Tokyo Medical and Dental University, 1-5-45 Yushima, Bunkyo-ku, Tokyo 113-8510, Japan and [3]Department of Pathology, Jikei University School of Medicine, 3-25-8 Nishi-Shimbashi, Minato-ku, Tokyo 105-8461, Japan

*To whom correspondence should be addressed. Tel: +81 4 7164 1111 ext. 6601; Fax: +81 4 7166 8638;
Email: atsubo@jikei.ac.jp

To identify key genes involved in the complex multistep process of hepatotumorigenesis, we reduced multivariate clinicopathological variables by using the Long–Evans Cinnamon rat, a model with naturally occurring and oxidative stress-induced hepatotumorigenesis. Gene expression patterns were analyzed serially by profiling liver tissues from rats of a naive status (4 weeks old), through to those with chronic hepatitis (26 and 39 weeks old) to tumor development (67 weeks old). Of 31 099 probe sets used for microarray analysis, 87 were identified as being upregulated in a stepwise manner during disease progression and tumor development. Quantitative real-time reverse transcription–polymerase chain reaction and statistical analyses verified that IQGAP1 and vimentin mRNA expression levels increased significantly throughout hepatotumorigenesis. A hierarchical clustering algorithm showed both genes clustered together and in the same cluster group. Immunohistochemical and western blot analyses showed similar increases in protein levels of IAGAP1 and vimentin. Finally, pathway analyses using text-mining technology with more comprehensive and recent gene–gene interaction data identified IQGAP1 and vimentin as important nodes in underlying gene regulatory networks. These findings enhance our understanding of the multistep hepatotumorigenesis and identification of target molecules for novel treatments.

Introduction

Primary liver cancer ranks third worldwide as a cause for cancer-related mortality, according to World Health Organization reports. The incidence is increasing even in low-endemic Western countries, with hepatocellular carcinoma (HCC) and cholangiocarcinoma accounting for most of these cases. The prognosis for advanced liver cancer remains very poor.

Recent advances in microarray technology have resulted in exponential accumulation of gene expression profiling data and provided novel insights into the molecular mechanisms underlying hepatotumorigenesis (1–3). Nevertheless, the molecular pathogenesis of liver cancer is difficult to establish, because patients present with highly variable clinicopathological features, the risk factors are diverse and liver cancer is heterogenous in nature, both pathologically and biologically (4–7). Such heterogeneity and variation probably underlies the genomic diversity of liver cancer, making it difficult to identify gene signatures in hepatotumorigenesis. In fact, gene expression profiling patterns of HCC differ even between patients with hepatitis B and C virus infections (8,9). Alternatively, it is unclear whether differences in gene expression between tumor and non-tumor tissues represent the cause or consequence of the neoplastic transformation because liver cancer generally evolves through multistep and diverse dysregulated molecular pathways (4).

Abbreviations: HCC, hepatocellular carcinoma; LEC, Long–Evans Cinnamon; RT–PCR, reverse transcription–polymerase chain reaction.

Liver cancer of any etiology is commonly preceded by chronic inflammation, which is linked tightly to oxidative stress (4,10,11). Indeed, oxidative stress is an important fundamental factor in tumorigenesis that is common to wide-ranging etiologies. For instance, oxidative stress promotes fibrogenesis, serves as an oncogenic mutational mechanism and might accelerate telomere shortening (4,12,13).

Long–Evans Cinnamon (LEC) rats with a genetic deletion in the copper-transporting *Atp7b* gene (14), which is homologous to Wilson's disease gene, exhibit accumulation of large amounts of copper in the liver and spontaneously develop chronic hepatitis, cholangiofibrosis and eventually liver tumor (15–17). Such excessive accumulation of transition metals causes chronic inflammation, characterized by excess production of reactive oxygen species (18), because transition metals interact with physiologically produced reactive oxygen species to catalyze the formation of highly cytotoxic hydroxyl radicals via the Fenton/Haber–Weiss reaction (19). Continuous oxidative stress conditions could be responsible for the pathological processes at play in hepatotumorigenesis (16). Thus, LEC rats could be a useful model to define the multistep mechanisms of hepatotumorigenesis induced by oxidative stress.

To elucidate the molecular mechanisms involved in the multistep hepatotumorigenesis, this study investigated genes that are upregulated in a stepwise manner from the naive liver condition to chronic oxidative stress-induced hepatitis and liver tumor by time-series microarray analysis. The time-dependent gene expression profile should reflect the multistep process of hepatotumorigenesis and identify genes that function specifically in this process. The study also undertook data mining to clarify the impact of candidate genes in the tumor-specific dysregulated gene networks using text-mining technology. These analyses would be helpful not only for a better understanding of the multistep process of liver tumor development but also to identify novel features of known genes and target molecules for treatment.

Materials and methods

Tissue samples

Four-week-old male LEC rats were purchased from Charles River Japan (Yokohama, Japan) and maintained in controlled environments. At 4, 26, 39 and 67 weeks of age, the rats were killed by exsanguination of blood from the abdominal aorta under pentobarbital anesthesia. Paired liver tumor and adjacent non-tumor tissue specimens were obtained from 67-week-old LEC rats ($n = 8$, Figure 1) that had developed liver tumors. Liver tissues without tumor were obtained from 4-, 26- and 39-week-old LEC rats ($n = 6$ for each) for analysis of the chronological changes in gene expression profiles. Long–Evans Agouti rats at 67 weeks of age ($n = 3$), which are wild-type rats, served as the control group (a kind gift from Dr Kozo Matsumoto, Tokushima University, Japan). The Committee for the Care and Use of Laboratory Animals of the Jikei University School of Medicine approved all experimental protocols.

Gene expression analysis

Total RNA was extracted from tissue samples using the RNeasy kit (QIAGEN, Valencia, CA). The RNA integrity was assessed using the Agilent 2100 BioAnalyzer (Agilent Technologies, Palo Alto, CA). A comprehensive gene expression analysis was then performed using 3 μg of total RNA from each sample and the GeneChip® Rat Genome 230 2.0 Array (Affymetrix, Santa Clara, CA) containing 31 099 probe sets, according to the instructions supplied by the manufacturer. To confirm the reproducibility of the results, in the first series of experiments (Figure 1), equivalent amounts of RNA from two pairs randomly selected from eight paired liver tumor and adjacent non-tumor tissue specimens were mixed and analyzed. The average gene expression levels for tumor and non-tumor tissue samples were calculated using the four microarray datasets, respectively. In the following experiments (Figure 1), a mixture of

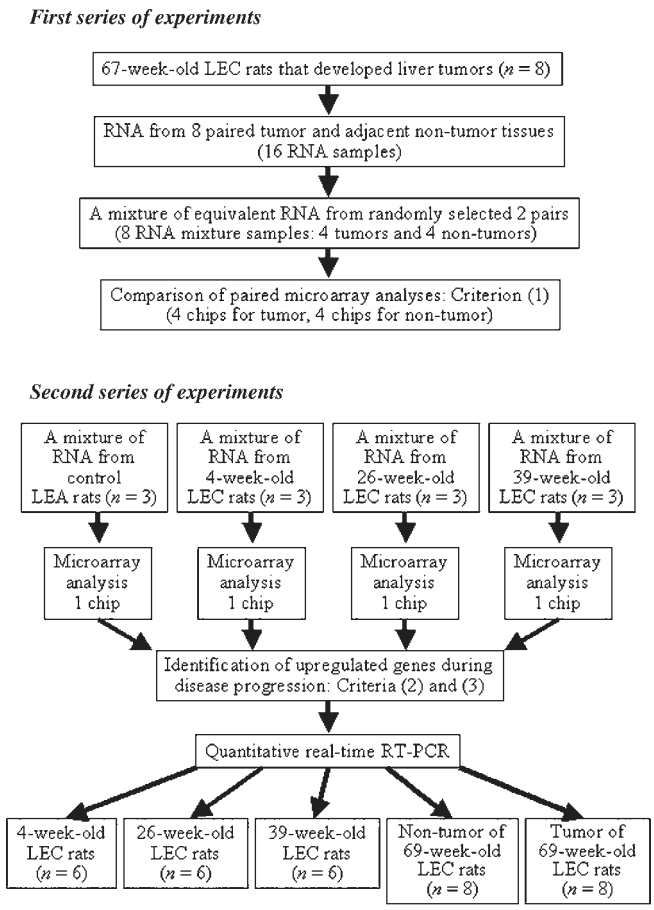

Fig. 1. Analysis flowchart for identification of stepwise upregulated genes during disease progression and multistep hepatotumorigenesis.

equivalent amounts of RNA isolated from LEC rats at 4, 26 and 39 weeks of age and controls ($n = 3$ for each), respectively, was exploited as an RNA pool for microarray analyses. Microarray datasets were normalized by the robust multi-array analysis, using the R 2.6.1 statistical software together with a BioConductor package (http://www.bioconductor.org/). Normalized expression levels were presented as $\log_2$-transformed values by robust multi-array analysis, and control probe sets were removed for further analysis. To eliminate background signals, genes were selected if their expression was assigned as 'Present' in at least one sample by the GeneChip Operating Software version 1.4 (Affymetrix). A total of 11 305 probes met the quality criteria in the first experiments and were thus subjected to further analysis.

Differential gene expression during disease progression

To identify genes that were upregulated during disease progression and involved in multistep hepatotumorigenesis, each gene was analyzed for fold change and statistical significance using the following three criteria: (i) >2-fold upregulation in tumor tissue samples compared with adjacent non-tumor tissue samples and P values < 0.01 (analyzed by two-tailed, paired t-test); (ii) stepwise increase in relative expression level at weeks 4, 26 and 39, as well as in non-tumor and tumor tissues at week 67 and (iii) relative expression levels at weeks 26 and 39 ('chronic oxidative stress-induced hepatitis phase') and in non-tumor tissue samples higher than the control sample ('no or less oxidative stress status'). The third criterion was important for selection of genes that were considered more strongly influenced by continuous oxidative stress. For paired t-test, false discovery rate was calculated using the Benjamini–Hochberg method. Three similar criteria were applied also to identify downregulated genes: (i) greater than a 2-fold downregulation in tumor tissues compared with adjacent non-tumor tissues and P values < 0.01; (ii) stepwise decrease in relative expression level at weeks 4, 26 and 39, as well as in non-tumor and tumor tissues at week 67 and (iii) relative expression levels at weeks 26 and 39 and in non-tumor tissue samples lower than the control.

Hierarchical clustering

Upregulated and downregulated probe sets were analyzed by hierarchical clustering using the R 2.6.1 statistical software. The gene expression intensities were transformed into Z scores to set the mean expression intensity to 0 and variance to 1 for all genes. Pearson's correlation coefficient was used to calculate a similarity matrix among probe sets. The complete linkage method was used for agglomeration.

Quantitative real-time reverse transcription–polymerase chain reaction

To validate microarray results and to confirm quantitatively any observed differences in gene expression level, each sample was also subjected to reverse transcription–polymerase chain reaction (RT–PCR) and quantitative real-time RT–PCR at least three times using an ABI PRISM 7700 Sequence Detection System (Applied Biosystems, Foster City, CA). Aliquots of RNA were mixed with oligo(dT) primer to obtain complementary DNA using reverse transcriptase. Target genes in the complementary DNA solution were amplified in a PCR mixture containing TaqMan Universal PCR Master Mix (Applied Biosystems), forward and reverse primers and TaqMan probes (Roche Diagnostics, Indianapolis, IN) designed by the Universal Probe Library Assay Design Center (http://www.roche-applied-science.com/sis/rtpcr/upl/adc.jsp). The expression levels of the 18S rat housekeeping gene were also quantified in all samples using the standard primers and TaqMan probe (Applied Biosystems). Differences in gene expression levels among week 4, 26 and 39 samples ($n = 6$ for each, Figure 1), as well as non-tumor and tumor tissues ($n = 8$ for both), were examined by one-way analysis of variance followed by Tukey test or Games–Howell procedure, as appropriate. Each dataset was evaluated for normality of distribution by the Shapiro–Wilk test. P values < 0.05 were considered significant. Statistical analyses were performed using the SPSS 17.0 statistical package (SPSS, Chicago, IL).

Immunohistochemistry

Formalin-fixed paraffin-embedded tissue sections were subjected to the streptavidin–biotin–peroxidase complex assay (i-VIEW DAB kit; Ventana Japan, Yokohama, Japan) on the Ventana auto-immunostaining system (Ventana Japan). Slides were pretreated by the recommended procedures for antigen retrieval. The sections were then incubated with rabbit polyclonal and monoclonal antibodies to IQGAP1 (H-109; Santa Cruz Biotechnology, Santa Cruz, CA) and vimentin (Epitomics, Burlingame, CA) at dilutions of 1:500 and 1:200, respectively, for 30 min at room temperature and then washed three times in phosphate-buffered saline. Sections were incubated with the appropriate secondary antibody for 30 min at room temperature.

Western blotting

Liver tissues were homogenized by sonication in lysis buffer. The protein concentration of each tissue lysate was determined using a bicinchoninic acid protein assay kit (Pierce, Rockford, IL). Samples were subjected to sodium dodecyl sulfate–polyacrylamide gel electrophoresis and then electrotransferred onto nitrocellulose membrane. Membranes were blocked with 5% non-fat milk and then probed with the above-described primary antibodies and another for β-actin (Abcam, San Diego, CA). The bound antibodies were visualized with horseradish peroxidase-conjugated secondary antibodies using Enhanced Chemiluminescence western blotting detection reagents (Amersham Pharmacia Biotech, Piscataway, NJ). The substrate reaction was recorded on X-ray film.

Bioinformatics

Pathway analysis was used to clarify the significance of candidate genes in the gene regulatory networks, using GENPAC® (NalaPro Technologies, Tokyo, Japan) and Cytoscape (http://www.cytoscape.org). GENPAC is a novel information extraction system and database for life science using natural language processing/text-mining technology, thereby deducing gene–gene interaction datasets (20). Cytoscape is a visualization and analysis tool for biological pathways (21). Gene ontology annotation was realized by using the GeneCodis 2.0 web tool (http://genecodis.dacya.ucm.es).

Expression of candidate genes in human microarray databases

To determine the expression levels of candidate genes in human liver cancer, we explored and analyzed publicly available microarray datasets of human liver cancer from the National Center for Biotechnology Information Gene Expression Omnibus (GEO: http://www.ncbi.nlm.nih.gov/geo/). For each microarray dataset, differences in the expression levels of candidate genes between human liver cancer and normal liver tissues were examined by Wilcoxon rank-sum test or one-sample t-test, as appropriate.

Results

Stepwise-upregulated genes during the development of liver tumor

Of the 11 305 probe sets filtered, 482 were initially identified as upregulated according to the first criterion of selection. Of these 482 probe sets, 122 met the second criterion. Finally, 87 probe sets (including 22 with no annotation) satisfied the third criterion for

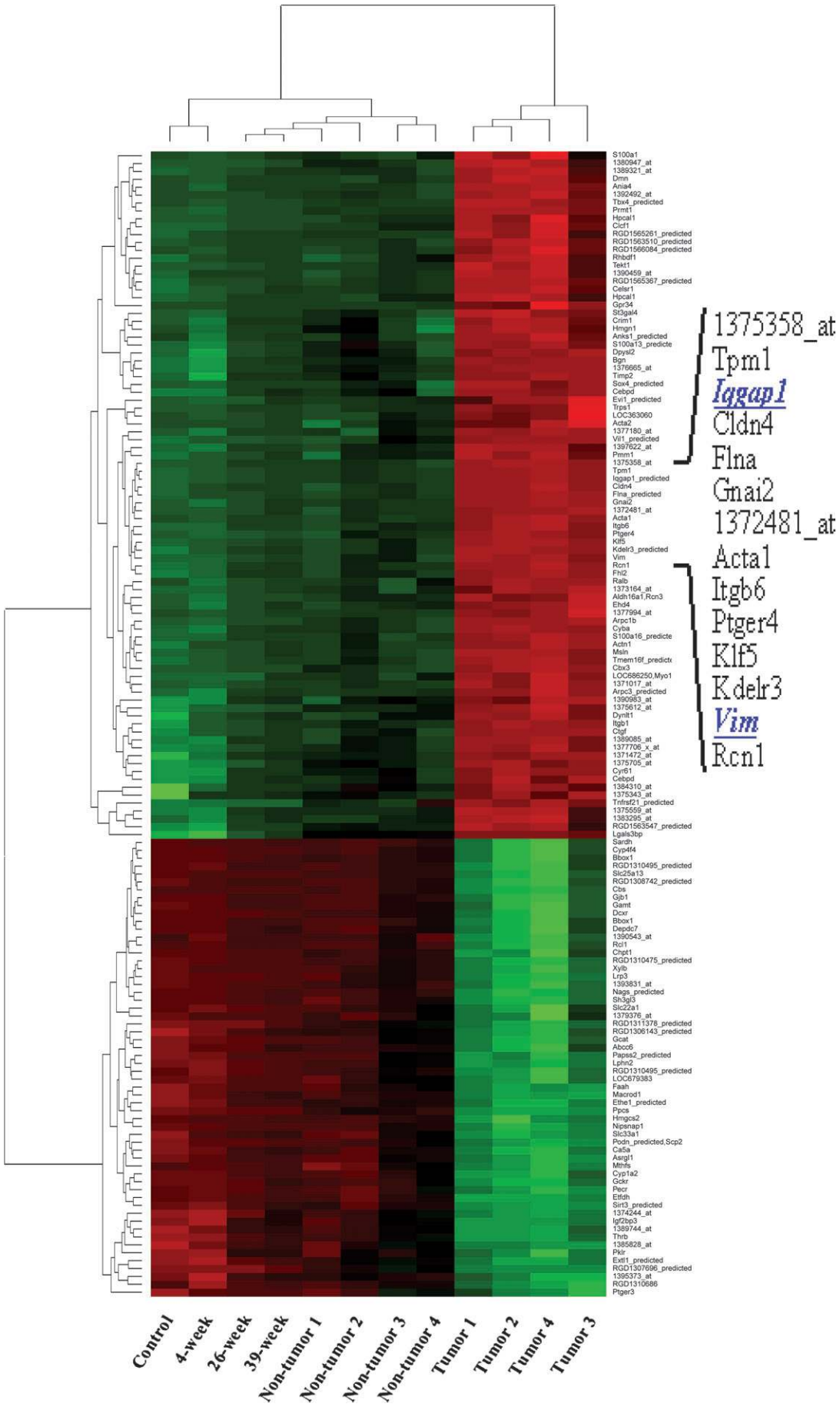

selection (supplementary Table 1 is available at *Carcinogenesis* Online). When the cut-off value for the paired *t*-test for 11 305 probe was set at $P < 0.01$, the estimated false discovery rate was 0.0273. The list contained genes associated with a variety of biological processes, such as cell/cell-matrix adhesion, signal transduction, positive regulation of cell proliferation, integrin-mediated signaling, angiogenesis, regulation of cell growth, positive regulation of the mitogen-activated protein (MAP) kinase kinase kinase cascade, cell motion and inflammatory response. All microarray data have been submitted to Gene Expression Omnibus as GSE17384 ('Gene expression data from the LEC rat model with naturally occurring and oxidative stress-induced liver tumorigenesis'; http://www.ncbi.nlm.nih.gov/geo/). The accession numbers for 'Non-tumor liver at 67 weeks_1 to _4', 'Control liver at 67 weeks', 'Liver at 4, 26 and 39 weeks' and 'Tumor liver at 67 weeks_1 to _4' are GSM434390-3, GSM434394, GSM434395-7 and GSM434398-401, respectively.

Stepwise downregulated genes during the development of liver tumor

Similarly, 58 probe sets (including 7 with no annotation) were identified as being stepwise downregulated during disease progression and tumorigenesis according to all selection criteria (supplementary Table 2 is available at *Carcinogenesis* Online). The list also included genes associated with a variety of molecular functions such as metal/iron ion binding, transferase activity, oxidoreductase activity, protein homodimerization and electron carrier activity.

Two-dimensional hierarchical clustering algorithm

Figure 2 represents the result of hierarchical clustering of the 87 upregulated and 58 downregulated probe sets. A two-dimensional hierarchical clustering algorithm completely distinguished between tumor and non-tumor tissues (Figure 2). The dendrogram shows that samples from 4-week-old LEC and control rats clustered together and formed a statistically different group from samples of 26-, 39- and 67-week-old rats (non-tumor and tumor), indicating that the listed genes were altered by persistent exposure to oxidative stress.

Validation of microarray data by quantitative real-time RT–PCR

To verify the reliability of the microarray data, all the 87 upregulated genes and all time-point samples of each gene were subjected to quantitative real-time RT–PCR. The average mRNA expression levels simply increased in a phased manner in only five genes: connective tissue growth factor (*CTGF*), IQ motif containing GTPase-activating protein 1 (*IQGAP1*), vimentin (*Vim*), smooth muscle alpha-actin (*Acta2*) and reticulocalbin 3 (*Rcn3*). The remaining 82 genes did not show a stepwise increase. Analysis of variance showed significant differences in expression of CTGF, IQGAP1 and vimentin. Finally, *post hoc* analyses showed significant increases in IQGAP1 and vimentin in a stepwise manner during liver disease progression and tumorigenesis (Figure 3). IQGAP1 mRNA levels (mean ± SD) were 0.17 ± 0.15, 0.76 ± 0.21, 1.43 ± 0.49, 2.74 ± 0.34 and 54.33 ± 12.60 in non-tumor liver tissue at week 4, 26, 39 and 67 and tumor tissues, respectively. Similarly, vimentin mRNA levels were 0.0011 ± 0.00035, 0.32 ± 0.08, 0.62 ± 0.28, 4.27 ± 1.92 and 40.78 ± 12.01. All comparisons between two time points except 26 week versus 39 week showed significantly different relative expression levels in both IQGAP1 and vimentin. IQGAP1 and vimentin clustered together and were in the same cluster group (Figure 2).

Immunohistochemical staining and western blot analysis

Next, the expressions of IQGAP1 and vimentin were assessed at the protein level during hepatotumorigenesis by immunohistochemical staining with antibodies against the two proteins (Figure 4A and B). Immunostaining for IQGAP1 and vimentin in the cell membrane or pericytoplasm gradually increased with time. The cytoplasm of hepatocytes and lymphocytes showed IQGAP1 staining and strongly immunopositive cells were observed in tumor tissues. Western blotting confirmed the immunostaining results for IQGAP1 and vimentin according to the stepwise progression of hepatocarcinogenesis (Figure 4C).

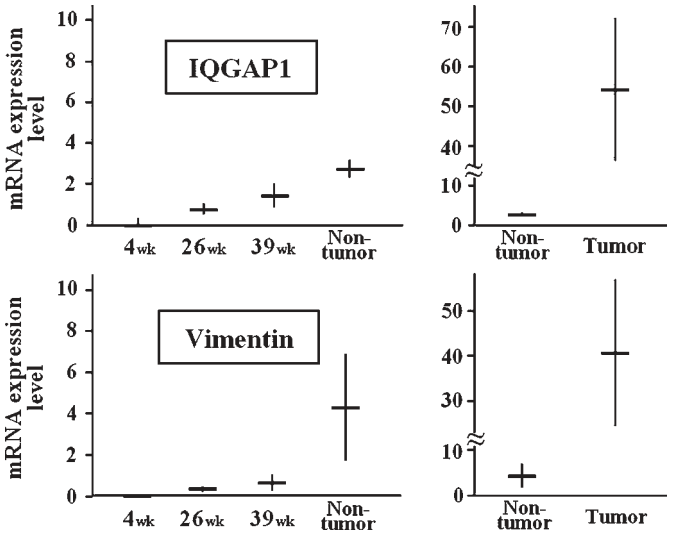

Fig. 3. Validation of differentially expressed genes using quantitative real-time RT–PCR analysis for IQGAP1 and vimentin. One-way analysis of variance and subsequent *post hoc* analyses showed that the expression levels of only two genes, IQGAP1 and vimentin, increased significantly in a stepwise manner during liver disease progression and tumorigenesis. All comparisons between two time points except 26 weeks versus 39 weeks were significantly different in relative expression levels of both IQGAP1 and vimentin ($P < 0.05$).

IQGAP1 and vimentin interact with other genes in gene regulatory networks

To provide insights into the relationship of *IQGAP1* and *vimentin* in underlying gene regulatory networks, microarray data and array-independent text mining were integrated by using GENEPAC and Cytoscape. Sixty-five upregulated known functional genes were related to another 470 genes and connected by 1009 interaction edges (supplementary Figure 1 is available at *Carcinogenesis* Online). *IQGAP1* and *vimentin* were identified as important nodes in the network graph and considered as key regulators. Figure 5A extracted from the interactive graph illustrates the direct relationship of *IQGAP1* and *vimentin* with 37 and 18 other regulatory genes, respectively, including *CDH1* (*E-cadherin*) connecting *IQGAP1* and *vimentin*.

We then explored the relationship of these genes to 'oxidative stress'-related, 'carcinogenesis/tumorigenesis'-related or 'fibrogenesis'-related genes. The number of genes that were related to each category and the degree of overlap between gene sets are shown in Figure 5B. Among 38 genes connected directly with *IQGAP1*, 31 and 31 were related to 'oxidative stress' and 'carcinogenesis/tumorigenesis', respectively. Twenty and 8 of 38 genes were associated with both and all categories, respectively. Among 19 genes connected directly with *vimentin*, 15 were related to 'oxidative stress' and 'carcinogenesis/tumorigenesis'. Five of 19 genes were associated with all categories.

IQGAP1 and vimentin in human liver cancer

IQGAP1 and vimentin were significantly upregulated in microarray datasets of human liver cancer (GSE 4108 and GSE14323). In the

Fig. 2. A two-dimensional hierarchical clustering algorithm of gene expression using probe sets for 87 upregulated and 58 downregulated genes. The horizontal and vertical axes of the dendrogram indicate the degree of similarity between genes and liver tissue samples, respectively, as determined by hierarchical clustering. The gene expression changes are presented in graduated color patches from green (least expression) to red (most abundant expression). IQGAP1 and vimentin were classified into the same cluster group. The vertical dendrogram reflects the clinical course during liver disease progression and tumorigenesis.

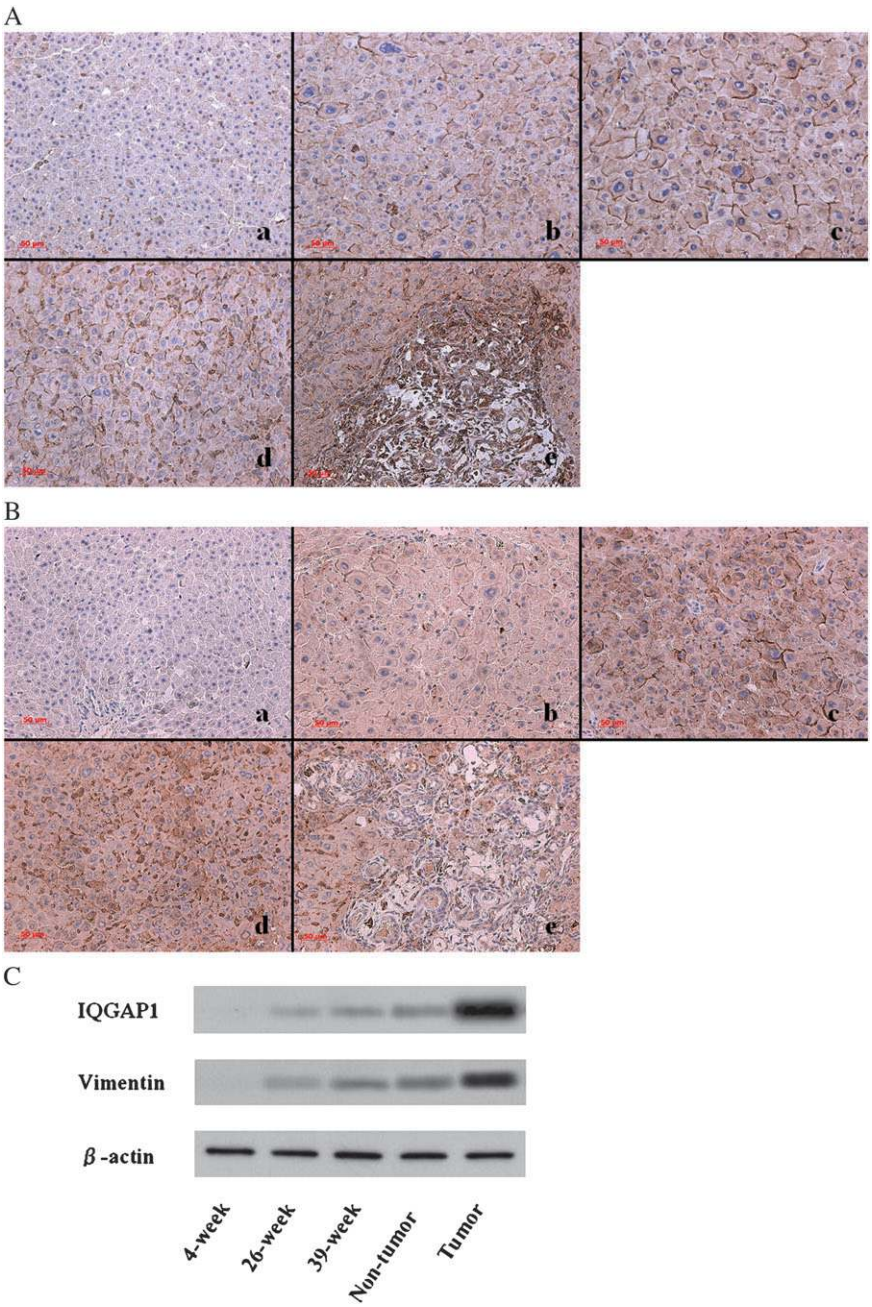

Fig. 4. Immunohistochemical reactivity and western blot analysis of IQGAP1 and vimentin in liver tissue from 4-, 26- and 39-week-old LEC rats (a, b and c), as well as in non-tumor (d) and tumor tissue (e) from 67-week-old LEC rats. (**A**) IQGAP1 staining was prominent at the cell–cell boundaries and cytoplasm according to the stepwise progression of hepatocarcinogenesis. (**B**) Vimentin staining was prominent at the cell–cell boundaries and cytoplasm according to the stepwise progression of hepatocarcinogenesis; bar = 50 μm. (**C**) Western blot analyses. β-Actin was also blotted, as a control. Results are representative data of at least three separate experiments.

GSE4108, the two genes were significantly upregulated in HCC, compared with normal liver tissue ($P = 1.76 \times 10^{-2}$ and 1.69×10^{-6}, respectively; supplementary Figure 2A is available at *Carcinogenesis* Online). In the GSE14323, the two genes were also significantly upregulated in HCC ($P = 7.43 \times 10^{-7}/5.02 \times 10^{-9}$ and 5.97×10^{-14}, respectively; supplementary Figure 2B is available at *Carcinogenesis* Online).

Discussion

To identify specific genes involved in multistep tumorigenesis, multivariate clinicopathological variables should be reduced and simple comparisons between tumor and non-tumor tissues should be avoided. Instead, in the present study, an animal model in which liver tumor developed naturally due to oxidative stress was prepared for microarray analysis to analyze serial changes in gene expression profiles from naive liver status to chronic hepatitis to tumor development. Such conditions or examinations cannot be reproduced or performed in human subjects. The analyses identified IQGAP1 and vimentin as stepwise-upregulated genes throughout the oxidative stress-induced process of hepatotumorigenesis, implicating both as reactive to persistent oxidative stress and important molecules in the mechanism of hepatotumorigenesis. In fact, the GEO database shows that IQGAP1 and vimentin are significantly upregulated in human HCC tissues (GSE4108 and

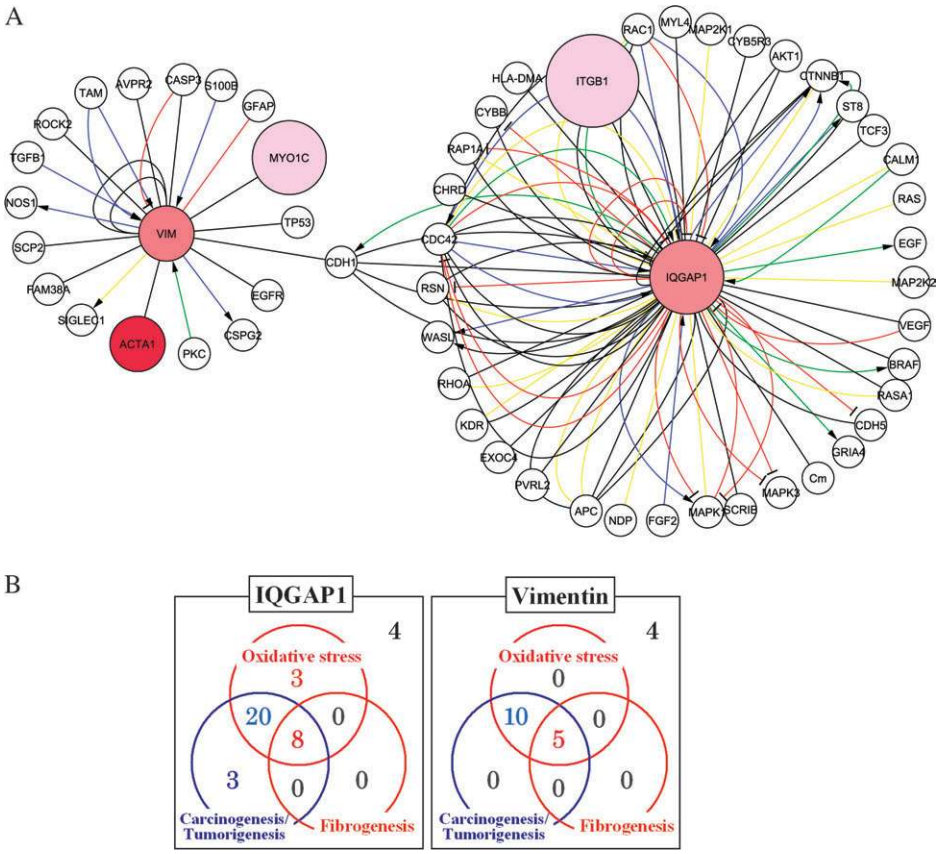

Fig. 5. *IQGAP1*, *vimentin* and related genes. (**A**) Part of the gene regulatory networks for *IQGAP1* and *vimentin*. Microarray data and array-independent text mining were integrated by gene regulatory network analysis (GENPAC). The interaction data were visualized and analyzed by Cytoscape. *CDH1* (*E-cadherin*) is directly linked to both *IQGAP1* and *vimentin*. Color nodes indicate relative overexpression of genes (fold change of tumor to non-tumor) on the microarray data: violet, 4> to ≥2; pale red, 16> to ≥4; red, ≥16 and white, 2> or no data. Node size indicates the proportion of the downstream effectors to the upstream modulators, of which genes are components of various signaling pathways. Edge colors and shapes reflect the interactions between genes: blue, upregulation type, such as 'activate'; red, downregulation type, such as 'inhibit'; green, regulation type, such as 'modulate' without information of up/downregulation; yellow, biochemical type, such as 'phosphorylation' and black, other types, such as 'associate'. (**B**) Biological backgrounds of genes linked directly to *IQGAP1* and *vimentin*. Among 38 genes linked directly to *IQGAP1*, 31 and 31 were related to 'oxidative stress' and 'carcinogenesis/tumorigenesis', respectively. Twenty and 8 of 38 genes were associated with both and all key words, respectively. Among 19 genes connected directly with *vimentin*, 15 were related to 'oxidative stress' and 'carcinogenesis/tumorigenesis'. Five of 19 genes were associated with all categories.

GSE14323, supplementary Figure 2 is available at *Carcinogenesis* Online), relative to other normal liver tissues. This was also confirmed in 165 of our patients with HCC ($P = 1.40 \times 10^{-4}$ and 4.97×10^{-3}, respectively; M.Kaoru and T.Hiroshi, unpublished data).

IQGAP1 is a scaffolding protein that specifically interacts with diverse proteins via multiple motifs. By doing so, IQGAP1 mediates multiprotein complex assembly and regulates multiple physiological cellular processes, such as cell–cell adhesion, cell polarization, cell migration, transcription and regulation of actin cytoskeleton formation and MAP kinase (MAPK) signaling. In addition, many IQGAP1-binding partners are implicated in tumorigenesis and/or tumor progression, including Rac1, Cdc42, Rap1, E-cadherin, β-catenin, components of the MAPK pathway, calmodulin, actin and APC (22–25). IQGAP1 is a downstream effector of Cdc42 and Rac1 (members of the Rho GTPase family). It localizes and interacts with the cytoplasmic domain of E-cadherin (CDH1), β-catenin (CTNNB1) and α-catenin at the cytoplasmic side of adherens junctions to negatively regulate E-cadherin-mediated cell–cell adhesion by interacting with β-catenin and dissociating α-catenin from the cadherin–catenin complex. Activated Cdc42 and Rac1 inhibit IQGAP1, thereby stabilizing the E-cadherin complex link to actin cytoskeleton and ensuring strong and rigid adhesion. Conversely, non-suppressed IQGAP1 results in diminished cell–cell adhesion (22,25,26). In human breast epithelial cells, IQGAP1 contributes to neoplastic transformation, upregulation of cell proliferation, angiogenesis, invasion and high metastatic capacity *in vitro*. Conversely, knockdown of IQGAP1 substantially reduces the amount of active Cdc42 and Rac1 in breast carcinoma *in vivo*. Cdc42/Rac1 and actin participate in IQGAP1-stimulated tumorigenesis, invasion and proliferation (27). In human gastric cancer, the expression levels of Rac1 and IQGAP1 are significantly correlated, while tumors showing E-cadherin mutations have reduced or absent levels of both (28). IQGAP1 also directly interacts with vascular endothelial growth factor type-2 receptor, via which reactive oxygen species derived from Rac1-dependent NAD(P)H oxidase are involved in vascular endothelial growth factor signaling, thereby promoting endothelial cell migration and proliferation that are important for angiogenesis (29). IQGAP1 activates B-Raf to mediate endothelial cell proliferation, which is essential for vascular endothelial growth factor to stimulate angiogenesis (30).

The IQGAP1 gene and/or protein is overexpressed in several human neoplasms: gastric (28,31,32), lung (33), colorectal (34), ovarian (35) and glioblastoma (36). From a clinical aspect, IQGAP1 seems closely associated with tumor invasion and metastasis and with the progression and poor prognosis of malignancies. However, it is not known whether IQGAP1 is the cause or consequence of neoplastic transformation. The present study analyzed the average levels of IQGAP1 mRNA and found increases of >4-fold, >8-fold and >16-fold in non-tumor liver tissues of rats at weeks 26, 39 and 67, respectively, compared with 4-week-old animals (Figure 3). This indicated that IQGAP1 expression was latently upregulated before development of the liver tumor. The immunohistochemical and western blotting results (Figure 4)

further supported that IQGAP1 is positively involved in the process of hepatotumorigenesis. This is the first report to document the stepwise increase of IQGAP1 mRNA and protein expression in a rat model of naturally occurring oxidative stress-induced hepatotumorigenesis. In *Iqgap2*$^{-/-}$ mice, HCC develops in an IQGAP1-dependent manner, while overexpression of IQGAP1 is associated with acquired β-catenin mutations, and dephosphorylated (active) β-catenin accumulates specifically in HCC livers but not in liver tissue from younger wild-type or *Iqgap2*$^{-/-}$ mice without HCC (37).

Vimentin is a cytoplasmic intermediate filament protein synthesized in cells of mesenchymal origin. It is therefore usually expressed in mesenchymal but not epithelial cells, and high vimentin expression in tumor epithelial cells has been correlated with tumorigenic potential, marked by the growth, invasive and migratory ability of cancer cells (38,39). Vimentin knockdown by RNA interference reduces cancer cell activities, resulting in greatly decreased tumorigenic potential (39,40). Reversal of the mesenchymal phenotype by inhibition of vimentin expression restores epithelial characteristics to cells *in vitro* (keratin gene expression) and smaller more differentiated tumors *in vivo* (39). Vimentin expression is also known as a sign of epithelial-to-mesenchymal transition, originally defined as the formation of mesenchymal cells from epithelia during the embryonic stages of development. In this process, the progression of tumors with strong malignant potential requires the epithelial phenotype to be lost along with junctional proteins such as E-cadherin and polarizing of the cells. Meanwhile, the cell acquires a more mesenchymal phenotype with reduced cell–cell adhesion, unpolarized spindle-shaped morphology (fibroblasts and fibroblast-like cells), enhanced cell motility and the presence of mesenchymal cellular markers such as vimentin (41,42).

In fact, advanced liver tumors in LEC rats spread over the liver in a scirrhous growth pattern and sometimes metastasize to lymph nodes. It is noteworthy that the expression levels of vimentin mRNA and protein increased in a stepwise manner during tumorigenesis in this study. Similar to IQGAP1, vimentin was latently upregulated before the development of liver tumors. It also increases in CCl_4-induced cirrhotic mouse livers, whereby hepatocytes derived from such livers and maintained *in vitro* exhibit high expression of vimentin and low expression E-cadherin, with the morphological characteristics of epithelial-to-mesenchymal transition (43). Prolonged exposure of mouse hepatocytes to transforming growth factor-β increases vimentin expression, suggesting that hepatocytes may have fibrogenic potential (44).

The text-mining software used in this study aimed to utilize more comprehensive and recent gene–gene interaction data (http://www.nalapro.com) than manual curation pathway databases, such as Ingenuity Pathway Analysis (45) and MetaCore (46). Moreover, the software provides interaction data with directional information among genes by using natural language processing/text-mining technology, unlike machine curation pathway databases, such as PubGene (47) and BiblioSphere (48), which use a different text-mining algorithm. Bioinformatics, such as integration of additional biological interactive data, is needed to uncover the molecular mechanisms underlying hepatotumorigenesis because the inherently complex and multivariate relations in gene regulatory network lead to difficulties in data interpretation.

In conclusion, IQGAP1 and vimentin were stepwise upregulated in an animal model with naturally occurring and oxidative stress-induced hepatotumorigenesis, implicating both as major molecules initiated and promoted by persistent oxidative stress, as key regulator genes involved in the multistep process of liver tumorigenesis and as targets for the development of novel gene therapies.

Supplementary material

Supplementary Tables 1 and 2 and Figures 1 and 2 can be found at http://carcin.oxfordjournals.org/

Funding

Grant-in-Aid for Scientific Research from the Ministry of Education, Culture, Sports, Science and Technology (Japan) (90322643 to A.T.).

Acknowledgements

We thank Ms Noriko Hashimoto (National Research Institute for Child Health and Development), Ms Mamiko Ohwada, Ms Rie Agata, Ms Yoko Yumoto and Mr Yasuo Mabashi (Jikei University School of Medicine) for the skillful technical assistance.

Conflict of Interest Statement: None declared.

References

1. Obama,K. *et al*. (2005) Genome-wide analysis of gene expression in human intrahepatic cholangiocarcinoma. *Hepatology*, **41**, 1339–1348.
2. Hass,H.G. *et al*. (2008) Identification of osteopontin as the most consistently over-expressed gene in intrahepatic cholangiocarcinoma: detection by oligonucleotide microarray and real-time PCR analysis. *World J. Gastroenterol.*, **14**, 2501–2510.
3. Iizuka,N. *et al*. (2008) Translational microarray systems for outcome prediction of hepatocellular carcinoma. *Cancer Sci.*, **99**, 659–665.
4. Farazi,P.A. *et al*. (2006) Hepatocellular carcinoma pathogenesis: from genes to environment. *Nat. Rev. Cancer*, **6**, 674–687.
5. Blechacz,B. *et al*. (2008) Cholangiocarcinoma: advances in pathogenesis, diagnosis, and treatment. *Hepatology*, **48**, 308–321.
6. Hammill,C.W. *et al*. (2008) Intrahepatic cholangiocarcinoma: a malignancy of increasing importance. *J. Am. Coll. Surg.*, **207**, 594–603.
7. Rosenthal,P. (2008) Hepatocarcinoma in viral and metabolic liver disease. *J. Pediatr. Gastroenterol. Nutr.*, **46**, 370–375.
8. Okabe,H. *et al*. (2001) Genome-wide analysis of gene expression in human hepatocellular carcinomas using cDNA microarray: identification of genes involved in viral carcinogenesis and tumor progression. *Cancer Res.*, **61**, 2129–2137.
9. Iizuka,N. *et al*. (2002) Comparison of gene expression profiles between hepatitis B virus- and hepatitis C virus-infected hepatocellular carcinoma by oligonucleotide microarray data on the basis of a supervised learning method. *Cancer Res.*, **62**, 3939–3944.
10. Schwarz,K.B. (1996) Oxidative stress during viral infection: a review. *Free Radic. Biol. Med.*, **21**, 641–649.
11. Shacter,E. *et al*. (2002) Chronic inflammation and cancer. *Oncology*, **16**, 217–226, 229; (discussion 230–232).
12. Marrogi,A.J. *et al*. (2001) Oxidative stress and p53 mutations in the carcinogenesis of iron overload-associated hepatocellular carcinoma. *J. Natl Cancer Inst.*, **93**, 1652–1655.
13. Kurz,D.J. *et al*. (2004) Chronic oxidative stress compromises telomere integrity and accelerates the onset of senescence in human endothelial cells. *J. Cell Sci.*, **117**, 2417–2426.
14. Wu,J. *et al*. (1994) The LEC rat has a deletion in the copper transporting ATPase gene homologous to the Wilson disease gene. *Nat. Genet.*, **7**, 541–545.
15. Masuda,R. *et al*. (1988) High susceptibility to hepatocellular carcinoma development in LEC rats with hereditary hepatitis. *Jpn. J. Cancer Res.*, **79**, 828–835.
16. Sone,K. *et al*. (1996) Inhibition of hereditary hepatitis and liver tumor development in Long-Evans cinnamon rats by the copper-chelating agent trientine dihydrochloride. *Hepatology*, **23**, 764–770.
17. Meerson,N.R. *et al*. (1998) Identification of B10, an alkaline phosphodiesterase of the apical plasma membrane of hepatocytes and biliary cells, in rat serum: increased levels following bile duct ligation and during the development of cholangiocarcinoma. *Hepatology*, **27**, 563–568.
18. Hensley,K. *et al*. (2000) Reactive oxygen species, cell signaling, and cell injury. *Free Radic. Biol. Med.*, **28**, 1456–1462.
19. Stohs,S.J. *et al*. (1995) Oxidative mechanisms in the toxicity of metal ions. *Free Radic. Biol. Med.*, **18**, 321–336.
20. Kushida,T. *et al*. (2009) *Collection of disease networks by hybrid curation method and the application for pathway analysis*. Proceedings of 2nd International Workshop on Intelligent Informatics in Biology and Medicine, 16–19 March 2009, Fukuoka, Japan, 800–806.
21. Shannon,P. *et al*. (2003) Cytoscape: a software environment for integrated models of biomolecular interaction networks. *Genome Res.*, **13**, 2498–2504.
22. Briggs,M.W. *et al*. (2003) IQGAP proteins are integral components of cytoskeletal regulation. *EMBO Rep.*, **4**, 571–574.
23. Mateer,S.C. (2003) IQGAPs: integrators of the cytoskeleton, cell adhesion machinery, and signaling networks. *Cell Motil. Cytoskeleton*, **55**, 147–155.
24. Noritake,J. *et al*. (2005) IQGAP1: a key regulator of adhesion and migration. *J. Cell Sci.*, **118**, 2085–2092.

25. Brown,M.D. (2006) IQGAP1 in cellular signaling: bridging the GAP. *Trends Cell Biol.*, **16**, 242–249.
26. Kuroda,S. *et al*. (1998) Role of IQGAP1, a target of the small GTPases Cdc42 and Rac1, in regulation of E-cadherin- mediated cell-cell adhesion. *Science*, **281**, 832–835.
27. Jadeski,L. *et al*. (2008) IQGAP1 stimulates proliferation and enhances tumorigenesis of human breast epithelial cells. *J. Biol. Chem.*, **283**, 1008–1017.
28. Walch,A. *et al*. (2008) Combined analysis of Rac1, IQGAP1, Tiam1 and E-cadherin expression in gastric cancer. *Mod. Pathol.*, **21**, 544–552.
29. Yamaoka-Tojo,M. *et al*. (2004) IQGAP1, a novel vascular endothelial growth factor receptor binding protein, is involved in reactive oxygen species—dependent endothelial migration and proliferation. *Circ. Res.*, **95**, 276–283.
30. Meyer,R.D. *et al*. (2008) IQGAP1-dependent signaling pathway regulates endothelial cell proliferation and angiogenesis. *PLoS ONE*, **3**, e3848; (1–11).
31. Sugimoto,N. *et al*. (2001) IQGAP1, a negative regulator of cell-cell adhesion, is upregulated by gene amplification at 15q26 in gastric cancer cell lines HSC39 and 40A. *J. Hum. Genet.*, **46**, 21–25.
32. Takemoto,H. *et al*. (2001) Localization of IQGAP1 is inversely correlated with intercellular adhesion mediated by e-cadherin in gastric cancers. *Int. J. Cancer*, **91**, 783–788.
33. Sun,W. *et al*. (2004) Identification of differentially expressed genes in human lung squamous cell carcinoma using suppression subtractive hybridization. *Cancer Lett.*, **212**, 83–93.
34. Nabeshima,K. *et al*. (2002) Immunohistochemical analysis of IQGAP1 expression in human colorectal carcinomas: its overexpression in carcinomas and association with invasion fronts. *Cancer Lett.*, **176**, 101–109.
35. Dong,P. *et al*. (2006) Overexpression and diffuse expression pattern of IQGAP1 at invasion fronts are independent prognostic parameters in ovarian carcinomas. *Cancer Lett.*, **243**, 120–127.
36. Balenci,L. *et al*. (2006) IQGAP1 protein specifies amplifying cancer cells in glioblastoma multiforme. *Cancer Res.*, **66**, 9074–9082.
37. Schmidt,V.A. *et al*. (2008) Development of hepatocellular carcinoma in Iqgap2-deficient mice is IQGAP1 dependent. *Mol. Cell. Biol.*, **28**, 1489–1502.
38. Bindels,S. *et al*. (2006) Regulation of vimentin by SIP1 in human epithelial breast tumor cells. *Oncogene*, **25**, 4975–4985.
39. Paccione,R.J. *et al*. (2008) Keratin down-regulation in vimentin-positive cancer cells is reversible by vimentin RNA interference, which inhibits growth and motility. *Mol. Cancer Ther.*, **7**, 2894–2903.
40. McInroy,L. *et al*. (2007) Down-regulation of vimentin expression inhibits carcinoma cell migration and adhesion. *Biochem. Biophys. Res. Commun.*, **360**, 109–114.
41. Thiery,J.P. (2002) Epithelial-mesenchymal transitions in tumour progression. *Nat. Rev. Cancer*, **2**, 442–454.
42. Huber,M.A. *et al*. (2005) Molecular requirements for epithelial-mesenchymal transition during tumor progression. *Curr. Opin. Cell Biol.*, **17**, 548–558.
43. Nitta,T. *et al*. (2008) Murine cirrhosis induces hepatocyte epithelial mesenchymal transition and alterations in survival signaling pathways. *Hepatology*, **48**, 909–919.
44. Kaimori,A. *et al*. (2007) Transforming growth factor-beta1 induces an epithelial-to-mesenchymal transition state in mouse hepatocytes *in vitro*. *J. Biol. Chem.*, **282**, 22089–22101.
45. Calvano,S.E. *et al*. (2005) A network-based analysis of systemic inflammation in humans. *Nature*, **437**, 1032–1037.
46. Ekins,S. *et al*. (2007) Pathway mapping tools for analysis of high content data. *Methods Mol. Biol.*, **356**, 319–350.
47. Jenssen,T.K. *et al*. (2001) A literature network of human genes for high-throughput analysis of gene expression. *Nat. Genet.*, **28**, 21–28.
48. Scherf,M. *et al*. (2005) The next generation of literature analysis: integration of genomic analysis into text mining. *Brief. Bioinform.*, **6**, 287–297.

Received April 23, 2009; revised December 7, 2009; accepted December 9, 2009